PAPER

Check for updates

Enhancing the HER rate over Pt–TiO$_2$ nanoparticles under controlled periodic illumination: role of light modulation†

Ettore Bianco,[a] Fabrizio Sordello, [ID][a] Francesco Pellegrino [ID] *[ab] and Valter Maurino [ID] *[ab]

In hydrogen production through water splitting, two reactions are involved: the hydrogen evolution reaction (HER) and oxygen evolution reaction (OER), both with efficiency issues. In previous works, our group demonstrated the possibility of enhancing H$_2$ production by conducting HCOOH photocatalytic reforming on metal–TiO$_2$ nanoparticles under controlled periodic illumination (CPI) rather than continuous illumination performed at the same average incident photon flux. The enhancement was observed only over specific metals, including Pt, Pd and Rh, due to their low Tafel slopes. Hydrogen adsorption and desorption energies are strongly dependent on the potential at the metal nanoparticles, and we demonstrated the ability to use CPI to induce oscillations in the potential of the catalyst. In this work, by modulating the duty cycle and the frequency of the CPI, we observed both of these playing a key role in boosting HER. Experimental evidence suggest that the relaxation of the photopotential during the dark period is the key factor for increasing the photonic efficiency of the reaction.

Introduction

Climate change has prompted the need to reconsider how we generate energy and products.[1–5] Scientists have spent many years researching different approaches to carrying out new sustainable reactions. In this situation, catalysis plays a crucial role.[6]

Of the different types of catalytic processes, those catalysed by light have attracted particularly considerable attention.[7–13] Despite sunlight being the most prevalent energy source on the planet, advancements in LED technology have enabled the development of more efficient devices for wider application, especially in photocatalysis, where the light absorption capabilities of the semiconductors can limit their ability to utilize sunlight.[14–16]

The effectiveness of catalysts/photocatalysts in accelerating multistep chemical process is limited when the rate determining step reaches the same rate as those of the other elementary reactions.[17] Various alternatives have been studied to further improve catalytic efficiency,[7,8] and among them, controlled periodic illumination (CPI) is gaining considerable attention for the investigation and optimization of the charge transfer mechanisms occurring under irradiation.[18–20]

CPI, depicted in Fig. 1, consists of modulating the light intensity according to a designed wave function, generally a square wave, to alternate light time (t_{ON}) and darkness time (t_{OFF}). The parameters that describe the square wave are duty cycle [$\gamma = t_{ON}/(t_{ON} + t_{OFF})$], frequency ($f = 1/$period) and photon flux during t_{ON} (I^{CPI}).

The hypothesis that applying CPI can improve photocatalytic efficiency was first proposed by Sczechowski et al.,[21] who observed an apparent five-fold increase in the photonic efficiency of formate oxidation under CPI compared to continuous illumination in concentrated TiO$_2$ suspensions. Although Stewart and Fox[22] confirmed this result, different studies later indicated that CPI is not able to work better than continuous illumination at the same average photonic flux incident on the sample.[20,23–30]

More recently, Ardagh et al.[31] theoretically demonstrated the possibility of boosting the rate of a catalyzed reaction through catalyst surface resonance—via the decoupling of chemical–physical steps which have different requirements in terms of interaction energies—with the boosting obtained by modulating (e.g. square wave) thermodynamic and kinetic-related properties of the catalyst/substrate couple. This effect can take place from 10 mHz up to 100 MHz, when the period of the applied waveform is comparable to the characteristic timescales of the individual micro-kinetic reaction steps.[19,31,32] In a recent work, the authors experimentally observed this effect in reforming of gas-phase methanol on Pt nanoparticles.[32]

a Department of Chemistry and NIS Centre, University of Torino, Via Giuria 7, 10125, Torino, Italy. E-mail: francesco.pellegrino@unito.it
b UniTo-ITT JointLab, University of Torino, Via Quarello 15/A, 10135, Torino, Italy
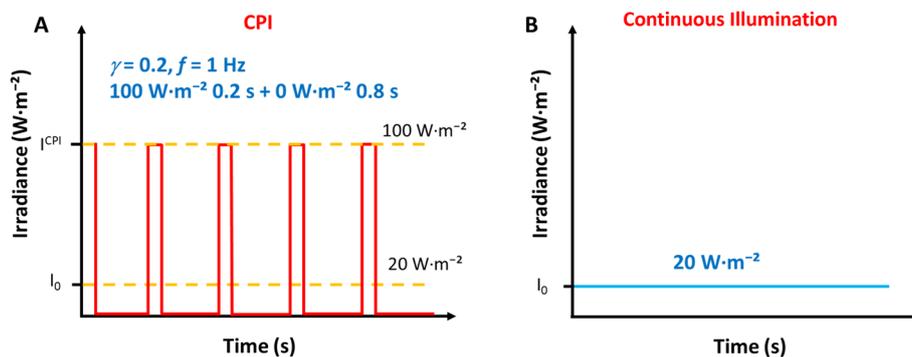† Electronic supplementary information (ESI) available. See DOI: https://doi.org/10.1039/d4cy00775a

This journal is © The Royal Society of Chemistry 2024

Catal. Sci. Technol., 2024, 14, 7205–7211 | 7205

Fig. 1 Light intensity during experiments performed under CPI (A) and continuous illumination (B) at certain conditions. I^{CPI} represents the irradiance at the peak of the square wave. During the tests, γ and f were changed so that the average incident irradiance (I_0) remains the same in the two different conditions.

In another recent paper, Sordello et al.[18] demonstrated the possibility of improving the HER efficiency on Pt–TiO$_2$ nanoparticles, by employing CPI instead of continuous illumination.

Moreover, we demonstrated an effect of the type of metal employed as a co-catalyst over TiO$_2$ bipyramidal nanoparticles. Although metal co-catalysts generally boost HER by extracting photogenerated electrons,[33–38] the enhancement under CPI is only possible with specific metals.[39]

Starting from this work, we systematically studied the effect of CPI parameters on the HER using Pt–TiO$_2$ nanoparticles (2% Pt loading on P25). Moreover, we further investigated the underlying mechanism by taking photocatalytic, electrochemical and photoelectrochemical measurements with Pt-P25 as well as Ag-P25 and bare P25, to test the various hypotheses previously made.
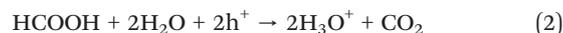
Results

As already mentioned, the purpose of this work is to evaluate the influence of γ and f on the HER under CPI. To verify the kinetic regime in a given range of irradiances, we first measured HER rates r_{HER} under continuous illumination at different incident light intensities on the top of a Pt–TiO$_2$ (P25) slurry (I_0: 10 W m^{-2}, 20 W m^{-2}, 40 W m^{-2}, 80 W m^{-2}, 100 W m^{-2} and 160 W m^{-2}). As shown in Fig. S4 of ESI,† a linear relationship between reaction rate and I_0 was observed, thus proving an absence of a variation in the kinetic regime when varying the incident light intensity in the spanned range.

To evaluate the role of parameters, we conducted several photocatalytic HER measurements over Pt–TiO$_2$ nanoparticles under different illumination conditions. TiO$_2$ was chosen because it is one of the most investigated semiconductor photocatalysts for photo-mediated hydrogen production.[37,40–45] Furthermore, P25, a benchmark in photocatalysis, has been extensively characterized in several reported works.[46–51]

Formic acid was employed as a hole scavenger (eqn (2)) due to its rapid oxidizing reaction over, TiO$_2$ even in anaerobic conditions, and hence the lack of any limitations on the proton reduction.[30,52] Moreover, it acts as a pH controller (eqn (1)), and the reaction (eqn (2)) does not generate intermediate species that can interfere with the HER.[53,54]

$$\text{Formic acid dissociation: HCOOH} \rightarrow \text{HCOO}^- + \text{H}^+ \quad (1)$$

$$\text{HCOOH} + 2\text{H}_2\text{O} + 2\text{h}^+ \rightarrow 2\text{H}_3\text{O}^+ + \text{CO}_2 \quad (2)$$

$$2\text{H}_3\text{O}^+ + 2\text{e}^- \rightarrow \text{H}_2 + 2\text{H}_2\text{O} \quad (3)$$

$$\text{HCOOH} \rightarrow \text{H}_2 + \text{CO}_2 \quad (4)$$

We compared r_{HER} in CPI and continuous illumination, varying the duty cycle from 0.1 to 0.8 (I_0 from 10 W m^{-2} to 80 W m^{-2}), and the frequency from 1 to 1000 Hz (see Fig. 2 and Table S1 in ESI†). The rates were calculated from the slope of the linear trend in H$_2$ photoproduction (see Fig. S4 to S7†). The increment was evaluated as the ratio of the rates (CPI vs. continuous illumination). Four sets of experiments were conducted, with the same average photon flux incident on the sample but different I_0 values (10, 20, 40, 80 W m^{-2}), as described in Table S1 in ESI.† Having observed no variation of the kinetic regime when varying the photon flow (Fig. S4†), a comparison of the different sets was thus possible. The synthesis of the catalyst is fully described in the Experimental section (ESI).†

As shown in Fig. 2, we observed a higher r_{HER} for almost all CPI experiments than for the continuous illumination, as obtained in a previous works.[18,39] This result was particularly pronounced above 1 Hz and for intermediate values of the duty cycle (γ = 0.2, γ = 0.4) (Fig. 2B), with a maximum r_{HER} observed at 10 Hz, followed in order by 100 Hz, 1000 Hz and 1 Hz. However, this trend did not hold for the other duty cycles, with small increases in reaction rate at γ = 0.1, and ones close to the experimental error at γ = 0.8.

To further investigate the effect of parameters, we performed a photoelectrochemical characterization of the Pt-P25 NP catalyst using open-circuit chronopotentiometry (Fig. 3) and chronoamperometry (Fig. S11 and S13†).
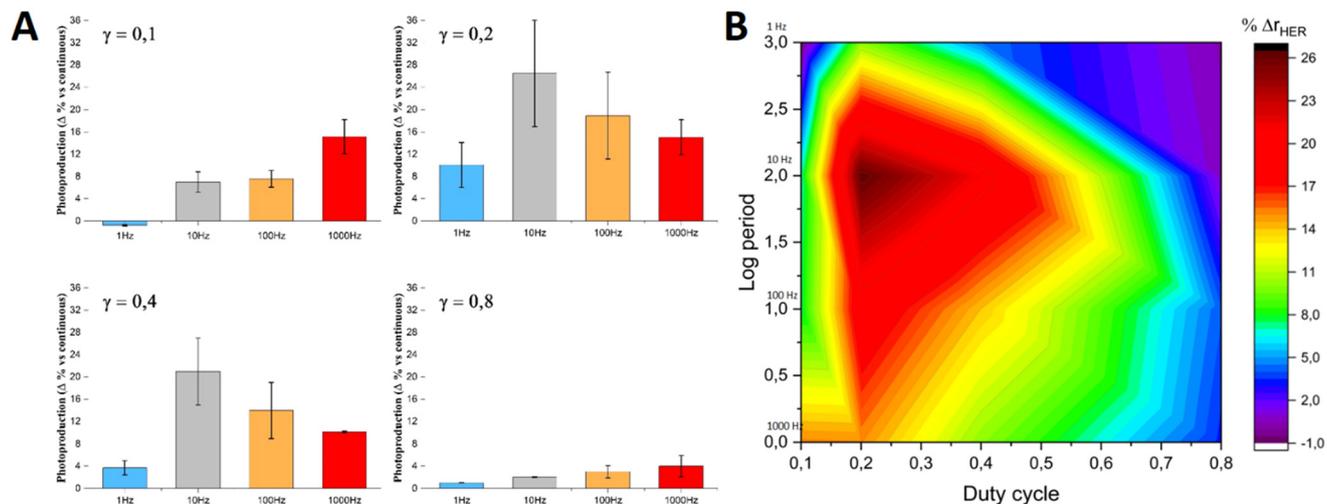
7206 | Catal. Sci. Technol., 2024, **14**, 7205–7211

This journal is © The Royal Society of Chemistry 2024

Fig. 2 (A) r_{HER} under CPI relative to continuous illumination at indicated duty cycles and frequencies over Pt-P25 catalyst. (B) Heat map showing the photocatalytic efficiency of Pt-P25 as a function of the duty cycle and the logarithm of the period (in ms). In the y axis is also reported the corresponding frequency.
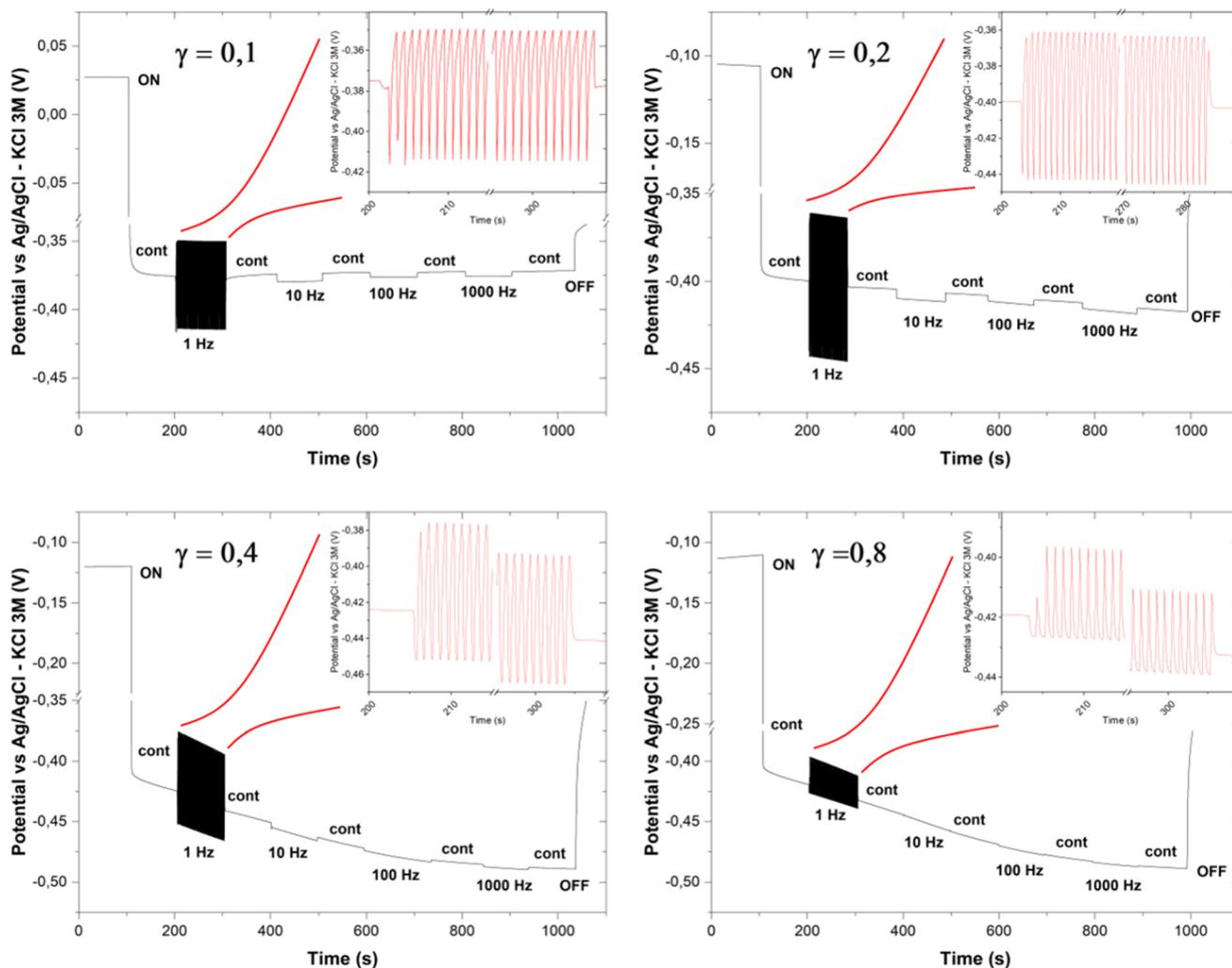

Fig. 3 OCP measurements under continuous illumination and CPI at indicated duty cycles and frequencies on Pt-P25. In the insets are highlighted the oscillations in potential registered at 1 Hz.

From a general point of view, under CPI, the open-circuit potential recorded was lower (more negative) than under continuous illumination, yielding a negative Δ_{OCP}. More specifically, at duty cycles of 0.1, 0.2 and 0.4, Δ_{OCP} values were larger than at 0.8, for which no significant OCP variation was recorded. Frequency did not significantly affect Δ_{OCP}: above 1 Hz, we measured similar voltage drops, whose amplitudes were found to depend on γ.

These results were fully consistent with the obtained r_{HER} (Fig. 2) and with photocurrent measurements on Pt-P25 (Fig. S11†), where we observed an increment of the photogenerated current (j) values at all duty cycles except 0.8, alongside low OCP values as previously discussed.

Concerning the dependence of photocurrent on frequency, at 1 Hz, we measured no difference in respect to continuous illumination. However, at 10 Hz, 100 Hz and 1000 Hz, higher values of j were observed under CPI, indicative of higher charge carrier density under these conditions (Fig. S11†). These results were also in accordance with r_{HER} data. However, it must be underscored that the results obtained from electrochemical analysis were only partially comparable to those obtained for the HER, due to the different systems employed (film *vs.* suspension) and the application of bias in the chronoamperometry measurements.

According to our hypothesis, CPI can induce an oscillation of catalyst–substrate interaction properties, hence alternately favoring different reaction steps that require mutually exclusive conditions. We suppose that during the light pulse, the surface potential became more negative, as effectively observed, so proton reduction to form Pt–H species was favored instead of H_2 desorption. In contrast, during the period of darkness, the potential became more positive, thus benefiting desorption of H_2 from the surface of the catalyst.

Due to the supposed relationship between surface–hydrogen (S–H) interaction and HER efficiency under CPI, we tested different interaction conditions by investigating Ag as a co-catalyst and bare TiO_2 (P25). Inspection of the volcano plot (Fig. 4B) showed Ag in the blue zone, where S–H interactions are weak and far from the optimum; thus, no significant improvement was expected under CPI, specifically

as the reaction being limited by the formation of S–H bonds, which can only occur during light time.

Additionally, due to the low hydrogen production and high sensitivity to oxygen, the reaction rates employing Ag–TiO_2 and bare TiO_2 were recorded only at $\gamma = 0.4$ and 100 Hz, because in these conditions, for Pt–TiO_2, we observed a significant increase in r_{HER} during CPI compared to continuous illumination.

As previously observed by Sordello et al.[39] with Ag–TiO_2 and bare TiO_2, r_{HER} was not affected by periodic illumination (Fig. 4A). However, under CPI, decreases in potential (Fig. S9 and S10†) and increases in photocurrent (Fig. S12 and S13†) were observed, similar to those registered in the presence of Pt–TiO_2.

As we believe that S–H interaction strength is influenced by oscillations in surface potential, we employed linear sweep voltammetry (LSV) on the three different catalysts to study the effect of the voltage decrease on the current density generated (Fig. 5).

A comparison of Tafel plots (Fig. 5B) showed a slope for Pt-P25 much less steep than those for Ag-P25 and bare P25, as already observed,[39] this indicates that any given increase in the potential applied would result in a larger increase in the generated current for Pt-P25 than for the other catalysts. In other words, the low voltage variations generated using CPI can affect r_{HER} more efficiently in the presence of Pt than in the presence of Ag or no co-catalyst. In the case of Pt–TiO_2, a 5 mV shift in overpotential would result in a 13.6% increase in current, *i.e.* r_{HER}. Considering Pt NPs deposited on TiO_2 as nanoelectrodes working at the potential imposed by the semiconductor, and as the Pt Tafel slope for the HER is reported to be only 30 mV per decade in literature,[56] the same potential shift would result in a 36% increase in current. Although we measured similar OCP variations for Ag–TiO_2 and bare TiO_2, these two catalysts presented Tafel slopes so steep that a decrease of 5 mV in the potential applied would produce a small 5.6% increase in the current.

Despite the OCP deviations at equilibrium being nearly the same for the three catalysts (for identical illumination conditions), when shifting from CPI to continuous illumination and reverse, the potential on Pt–TiO_2 would move almost
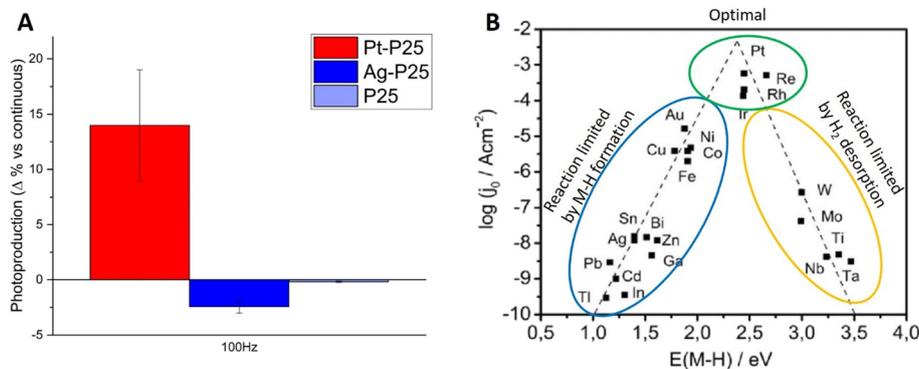

Fig. 4 r_{HER} relative to continuous illumination on Pt-P25, Ag-P25 and P25 (A). Schematic representation of the volcano plot (B) showing exchange current density as a function of the metal–H interaction strength; adapted from ref. 55.
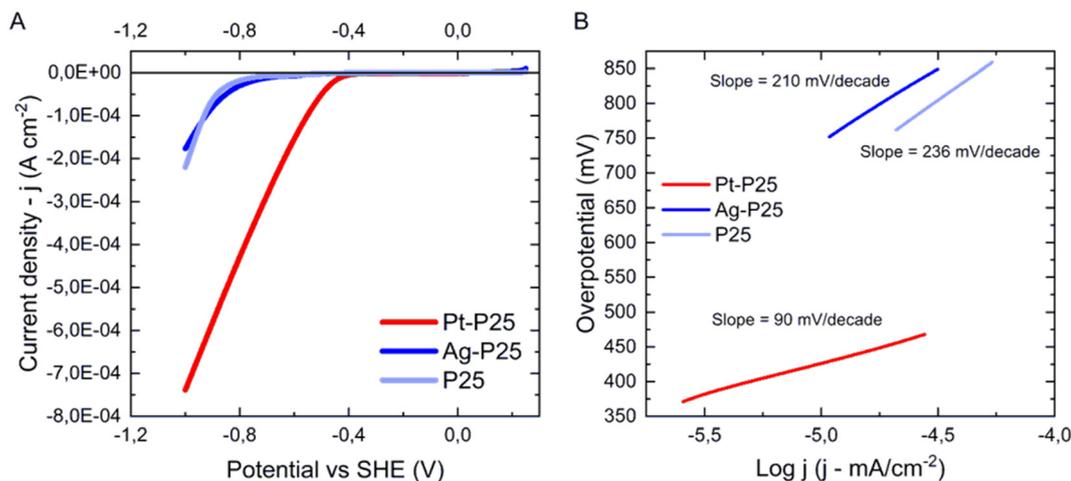
7208 | *Catal. Sci. Technol.*, 2024, **14**, 7205–7211

This journal is © The Royal Society of Chemistry 2024

Fig. 5 LSV (A) and Tafel plot (B) values for Pt-P25, Ag-P25 and bare P25.

instantaneously, while in the other two cases the movement would be slower. Moreover, at 1 Hz, we were able to track fluctuations in potential due to the alternating of light and darkness. For these oscillations, the range spanned in the presence of Pt–TiO$_2$ was found to be much larger (30–70 mV), suggesting that the response of the potential, due to variations in light intensity reaching the photocatalyst, is much more rapid on Pt-P25 than on Ag-P25 and P25.

Discussion

Our observations can be reasonably explained by the mechanism of surface catalytic resonance, theorized by Ardagh *et al.*[31] The oscillating potential of the surface of the catalyst enables the system to surpass the optimum efficiency achievable under static conditions. We suppose that the absence of a rate increase at duty cycles close to 1 and the limited increases at duty cycles close to 0, are related to variations in the amplitude of the voltage. In the first case, we suppose that the negative potential deviation occurring during the illumination pulse cannot be completely restored during the period of darkness, therefore resulting a slow desorption of hydrogen (Fig. 6, center). In contrast, for a

small duty cycle (*e.g.* equal to 0.1), proton reduction is hindered because the low negative potential variation produced during the light pulse cannot compensate for the positive deviation occurring during the period of darkness. As a consequence, for a significant amount of time, the charge carrier density is low and close to that in dark conditions, as depicted in Fig. 6 (right).

By investigating different co-catalysts, we have also confirmed that in the case of P25 the S–H interaction is a key factor in establishing the impact of CPI on r_{HER}. When the S–H interaction is weak, OCP variations under CPI cannot significantly influence hydrogen production, as confirmed by the steep Tafel slopes measured for Ag-P25 and bare P25. Further experimental evidence is provided by the voltage oscillations recorded during chronopotentiometry at 1 Hz. The amplitude of these oscillations is larger for Pt-P25 than for Ag-P25 and bare P25, for which the amplitudes are in fact negligible, as shown in Fig. 3, S8 and S9,† matching the r_{HER} results. We attribute these findings to the reactivity of the photocatalyst and hence its ability to alter its potential in response to variations in light intensity. Moreover, Pt undergoes a Tafel path, while Ag a Heyrovsky one. The Tafel step does not involve an electron transfer; therefore, it can
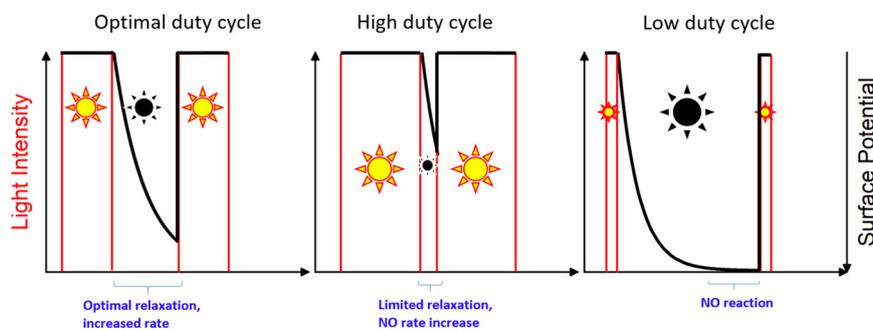

Fig. 6 Schematic representation of the different potentials at the nanoparticle surface as function of time during irradiation for the different duty cycles. The right axis is reversed so that the potential (shown in black) becomes more negative when increasing the signal strength.

This journal is © The Royal Society of Chemistry 2024

Catal. Sci. Technol., 2024, **14**, 7205–7211 | **7209**

work also during a period of darkness. Conversely, the Heyrovsky step (with an Eley–Rideal mechanism) provides a second electron transfer, preventing the HER in the absence of light. The mechanism here proposed is fully consistent with the experimental evidences, and further details on the possible mechanism beyond this behavior were already assessed in a recent paper.[39]

Conclusions

This work demonstrates the dependence of HER rate under CPI on frequency and duty cycle when using a $Pt–TiO_2$ catalyst, with this dependence also reflected in the current density increase and the OCP decrease. CPI is able to increase the photonic efficiency of formic acid photoreforming on suspended $Pt–TiO_2$ nanoparticles compared with continuous illumination. The efficiency increase seems to be related to the ratio of the duration of illumination to that of darkness, which may affect the relaxation of the potential after the light pulse, as illustrated in Fig. 6. Moreover, the Tafel slope of the catalyst system influences the response to oscillations in potential. It seems that only those systems that follow a Volmer–Tafel mechanism are able to profitably exploit the relaxation during the period of darkness.

CPI has been proven to be a useful tool not only for increasing photonic efficiency but also for studying the thermodynamics and the kinetics of surface photoinduced processes involving a catalyst/co-catalyst couple, thereby providing a deeper comprehension of photogenerated charge transfer and hydrogen evolution mechanisms.

Data availability

The data supporting this article have been included as part of the ESI.†

Conflicts of interest

There are no conflicts to declare.

Acknowledgements

Notes and references

1 N. Armaroli and V. Balzani, *Chem. – Asian J.*, 2011, **6**, 768–784.

2 C. D. Koolen and G. Rothenberg, *ChemSusChem*, 2019, **12**, 164–172.

3 J. Rockström, W. Steffen, K. Noone, Å. Persson, F. S. Chapin, E. F. Lambin, T. M. Lenton, M. Scheffer, C. Folke, H. J. Schellnhuber, B. Nykvist, C. A. de Wit, T. Hughes, S. van der Leeuw, H. Rodhe, S. Sörlin, P. K. Snyder, R. Costanza, U. Svedin, M. Falkenmark, L. Karlberg, R. W. Corell, V. J. Fabry, J. Hansen, B. Walker, D. Liverman, K. Richardson, P. Crutzen and J. A. Foley, *Nature*, 2009, **461**, 472–475.

4 P. C. K. Vesborg and T. F. Jaramillo, *RSC Adv.*, 2012, **2**, 7933–7947.

5 N. Armaroli and V. Balzani, *Angew. Chem., Int. Ed.*, 2007, **46**, 52–66.

6 C. R. Catlow, M. Davidson, C. Hardacre and G. J. Hutchings, *Philos. Trans. R. Soc., A*, 2016, **374**, 20150089.

7 N. Fajrina and M. Tahir, *Int. J. Hydrogen Energy*, 2019, **44**, 540–577.

8 M. Z. Rahman, F. Raziq, H. Zhang and J. Gascon, *Angew. Chem., Int. Ed.*, 2023, e202305385.

9 H. Nishiyama, T. Yamada, M. Nakabayashi, Y. Maehara, M. Yamaguchi, Y. Kuromiya, Y. Nagatsuma, H. Tokudome, S. Akiyama, T. Watanabe, R. Narushima, S. Okunaka, N. Shibata, T. Takata, T. Hisatomi and K. Domen, *Nature*, 2021, **598**, 304–307.

10 K. C. Christoforidis and P. Fornasiero, *ChemCatChem*, 2017, **9**, 1523–1544.

11 M. G. Walter, E. L. Warren, J. R. McKone, S. W. Boettcher, Q. X. Mi, E. A. Santori and N. S. Lewis, *Chem. Rev.*, 2010, **110**, 6446–6473.

12 H. Enzweiler, P. H. Yassue-Cordeiro, M. Schwaab, E. Barbosa-Coutinho, M. H. N. Olsen Scaliante and N. R. C. Fernandes, *J. Photochem. Photobiol., A*, 2020, **388**, 112051.

13 N. L. Reddy, S. Kumar, V. Krishnan, M. Sathish and M. V. Shankar, *J. Catal.*, 2017, **350**, 226–239.

14 F. K. Yam and Z. Hassan, *Microelectron. J.*, 2005, **36**, 129–137.

15 M. Bessho and K. Shimizu, *Electron. Commun. Jpn.*, 2012, **95**, 1–7.

16 O. Tokode, R. Prabhu, L. A. Lawton and P. K. J. Robertson, in *Environmental Photochemistry Part III*, ed. D. W. Bahnemann and P. K. J. Robertson, Springer Berlin Heidelberg, Berlin, Heidelberg, 2015, pp. 159–179, DOI: **10.1007/698_2014_306**.

17 E. Roduner, *Chem. Soc. Rev.*, 2014, **43**, 8226–8239.

18 F. Sordello, F. Pellegrino, M. Prozzi, C. Minero and V. Maurino, *ACS Catal.*, 2021, **11**, 6484–6488.

19 J. Qi, J. Resasco, H. Robatjazi, I. B. Alvarez, O. Abdelrahman, P. Dauenhauer and P. Christopher, *ACS Energy Lett.*, 2020, **5**, 3518–3525.

20 O. Tokode, R. Prabhu, L. A. Lawton and P. K. J. Robertson, *J. Photochem. Photobiol., A*, 2016, **319**, 96–106.

21 J. G. Sczechowski, C. A. Koval and R. D. Noble, *J. Photochem. Photobiol., A*, 1993, **74**, 273–278.

22 G. Stewart and M. A. Fox, *Res. Chem. Intermed.*, 1995, **21**, 933–938.

23 K. J. Buechler, T. M. Zawistowski, R. D. Noble and C. A. Koval, *Ind. Eng. Chem. Res.*, 2001, **40**, 1097–1102.

24 K. J. Buechler, C. H. Nam, T. M. Zawistowski, R. D. Noble and C. A. Koval, *Ind. Eng. Chem. Res.*, 1999, **38**, 1258–1263.

25 C. J. G. Cornu, A. J. Colussi and M. R. Hoffmann, *J. Phys. Chem. B*, 2001, **105**, 1351–1354.

26 C. Y. Wang, R. Pagel, J. K. Dohrmann and D. W. Bahnemann, *C. R. Chim.*, 2006, **9**, 761–773.

27 C. Y. Wang, R. Pagel, D. W. Bahnemann and J. K. Dohrmann, *J. Phys. Chem. B*, 2004, **108**, 14082–14092.

28 H. W. Chen, Y. Ku and A. Irawan, *Chemosphere*, 2007, **69**, 184–190.

29 O. I. Tokode, R. Prabhu, L. A. Lawton and P. K. J. Robertson, *J. Catal.*, 2012, **290**, 138–142.

30 M. Prozzi, F. Sordello, S. Barletta, M. Zangirolami, F. Pellegrino, A. B. Prevot and V. Maurino, *ACS Catal.*, 2020, **10**, 9612–9623.

31 M. A. Ardagh, O. A. Abdelrahman and P. J. Dauenhauer, *ACS Catal.*, 2019, **9**, 6929–6937.

32 M. Shetty, A. Walton, S. R. Gathmann, M. A. Ardagh, J. Gopeesingh, J. Resasco, T. Birol, Q. Zhang, M. Tsapatsis, D. G. Vlachos, P. Christopher, C. D. Frisbie, O. A. Abdelrahman and P. J. Dauenhauer, *ACS Catal.*, 2020, **10**, 12666–12695.

33 Z. H. N. Al-Azri, W.-T. Chen, A. Chan, V. Jovic, T. Ina, H. Idriss and G. I. N. Waterhouse, *J. Catal.*, 2015, **329**, 355–367.

34 C. Xia, T. Hong Chuong Nguyen, X. Cuong Nguyen, S. Young Kim, D. L. T. Nguyen, P. Raizada, P. Singh, V.-H. Nguyen, C. Chien Nguyen, V. Chinh Hoang and Q. Van Le, *Fuel*, 2022, **307**, 121745.

35 P. D. Tran, L. Xi, S. K. Batabyal, L. H. Wong, J. Barber and J. S. Chye Loo, *Phys. Chem. Chem. Phys.*, 2012, **14**, 11596–11599.

36 D. Wang and X.-Q. Gong, *Nat. Commun.*, 2021, **12**, 158.

37 M. Anpo and M. Takeuchi, *J. Catal.*, 2003, **216**, 505–516.

38 M. Ni, M. K. H. Leung, D. Y. C. Leung and K. Sumathy, *Renewable Sustainable Energy Rev.*, 2007, **11**, 401–425.

39 F. Sordello, M. Prozzi, V.-D. Hodoroaba, J. Radnik and F. Pellegrino, *J. Catal.*, 2024, **429**, 115215.

40 U. Diebold, *Surf. Sci. Rep.*, 2003, **48**, 53–229.

41 I. Ali, M. Suhail, Z. A. Alothman and A. Alwarthan, *RSC Adv.*, 2018, **8**, 30125–30147.

42 X. Chen and S. S. Mao, *Chem. Rev.*, 2007, **107**, 2891–2959.

43 G. Li, S. Ciston, Z. V. Saponjic, L. Chen, N. M. Dimitrijevic, T. Rajh and K. A. Gray, *J. Catal.*, 2008, **253**, 105–110.

44 A. Fujishima and K. Honda, *Nature*, 1972, **238**, 37–38.

45 Y. Sasaki, A. Iwase, H. Kato and A. Kudo, *J. Catal.*, 2008, **259**, 133–137.

46 E. P. Melián, C. R. López, A. O. Méndez, O. G. Díaz, M. N. Suárez, J. M. Doña Rodríguez, J. A. Navío and D. Fernández Hevia, *Int. J. Hydrogen Energy*, 2013, **38**, 11737–11748.

47 M. C. Hidalgo, M. Maicu, J. A. Navío and G. Colón, *Catal. Today*, 2007, **129**, 43–49.

48 D. Benz, K. M. Felter, J. Köser, J. Thöming, G. Mul, F. C. Grozema, H. T. Hintzen, M. T. Kreutzer and J. R. van Ommen, *J. Phys. Chem. C*, 2020, **124**, 8269–8278.

49 D. M. Tobaldi, R. C. Pullar, M. P. Seabra and J. A. Labrincha, *Mater. Lett.*, 2014, **122**, 345–347.

50 B. Abida, L. Chirchi, S. Baranton, T. W. Napporn, H. Kochkar, J.-M. Léger and A. Ghorbel, *Appl. Catal., A*, 2011, **106**, 609–615.

51 A. Kubiak, *Sci. Rep.*, 2024, **14**, 13827.

52 J. T. Schneider, D. S. Firak, R. R. Ribeiro and P. Peralta-Zamora, *Phys. Chem. Chem. Phys.*, 2020, **22**, 15723–15733.

53 L.-F. Liao, W.-C. Wu, C.-Y. Chen and J.-L. Lin, *J. Phys. Chem. B*, 2001, **105**, 7678–7685.

54 D. S. Muggli and M. J. Backes, *J. Catal.*, 2002, **209**, 105–113.

55 S. Trasatti, *J. Electroanal. Chem. Interfacial Electrochem.*, 1972, **39**, 163–184.

56 A. P. Murthy, J. Theerthagiri and J. Madhavan, *J. Phys. Chem. C*, 2018, **122**, 23943–23949.

This journal is © The Royal Society of Chemistry 2024

Catal. Sci. Technol., 2024, **14**, 7205–7211 | **7211**